DYE ADSORPTION USING XANTHAN GUM & LIGNIN-BASED CHEMICALLY CROSSLINKED HYDROGELS

A PROJECT REPORT

SUBMITTED IN PARTIAL FULFILLMENT OF THE REQUIREMENTS

FOR THE AWARD OF THE DEGREE

OF

MASTER IN SCIENCE

IN

CHEMISTRY

Submitted by

AKSHITA SRIVASTAVA

2K21/MSCCHE/05

Under the supervision of

Prof. Rajinder K. Gupta

DEPARTMENT OF APPLIED CHEMISTRY

DELHI TECHNOLOGICAL UNIVERSITY

(Formerly Delhi College of Engineering)

Bawana Road, Delhi-110042

May, 2023

DEPARTMENT OF APPLIED CHEMISTRY

DELHI TECHNOLOGICAL UNIVERSITY

(Formerly Delhi College of Engineering)

Bawana Road, Delhi-110042

CANDIDATE'S DECLARATION

I, Akshita Srivastava, Roll No. 2K21/MSCCHE/05 student of MSc (Chemistry), hereby declare that the project Dissertation titled "**Dye Adsorption using Xanthan Gum & Lignin-based Chemically Crosslinked Hydrogels**" which is submitted by me to the Department of Applied Chemistry, Delhi Technological University, Delhi in partial fulfilment of the requirement for the award of the degree of Master of Science, is original and not copied from any source without proper citation. This work has not previously formed the basis for the award of any Degree, Diploma Associateship, Fellowship, or other similar title or recognition.

Place- Delhi AKSHITA SRIVASTAVA

Date- May 31, 2023

DEPARTMENT OF APPLIED CHEMISTRY

DELHI TECHNOLOGICAL UNIVERSITY

(Formerly Delhi College of Engineering)

Bawana Road, Delhi-110042

CERTIFICATE

This is to ensure that the work introduced in this significant task report entitled "**Dye Adsorption using Xanthan Gum & Lignin-based Chemically Crosslinked Hydrogels**" which is submitted by **Akshita Srivastava, Roll No. 2K21/MSCCHE/05**, Department of Applied Chemistry, Delhi Technological University, Delhi in partial fulfilment of the requirement for the award of the degree of Master in Science (Chemistry) is a record of a project work carried out by the student under my supervision. To the best of my knowledge, this work has not been submitted in part or full for any Degree or Diploma to this University or elsewhere.

Prof. Rajinder K. Gupta

(Supervisor)

ACKNOWLEDGEMENT

The success and final outcome of this project required a lot of guidance and assistance from many people and I am extremely fortunate to have got this all along the completion of this project work. I wish to express my gratitude towards my project supervisor, Prof. Rajinder K. Gupta, Department of Applied Chemistry, Delhi Technological University, who gave me a golden opportunity to work under their guidance. Their scholastic guidance and sagacious suggestions helped me to complete the project on time. I wish to thank, Prof. Anil Kumar, Head of the Department of Applied Chemistry, Delhi Technological University, for his constant motivation and for providing able guidance. I am thankful and fortunate enough to get constant encouragement, support, and guidance from all teaching and non-teaching staff of the Department of Applied Chemistry, which helped me successfully complete my project work. I am also thankful to PhD scholars Ms. Manu, Mrs. Meenakshi Tanwar, and Ms. Ritu Sharma for their constant support and motivation. Finally, yet importantly, I would like to express my heartfelt thanks to my beloved family and friends who have endured my long working hours and whose motivation kept me going.

AKSHITA SRIVASTAVA

2K21/MSCCHE/05

ABSTRACT

The present study focuses on the synthesis of Xanthan Gum (XG-g-PAAcoAM), Lignosulphonate sodium salt (LS-g-PAAcoAM), and their combination (XG/LS-g-PAAcoAM) based hydrogels by grafting them onto acrylic acid and acrylamide. These hydrogels were investigated for their effectiveness in removing dyes from textile industries. The results demonstrate the reliability of the hydrogels, achieving a removal rate of over 91% when a dosage of 0.2 g was used in a 20 ml solution of Methylene blue dye over a period of 7 hours. The hydrogels have been characterized by using Fourier Transform Infrared Spectroscopy, Scanning Electron Microscopy, Thermogravimetric Analysis, and X-ray Diffraction Analysis. The adsorption behaviour of hydrogels was analysed using three common isotherm models: Langmuir, Freundlich, and Temkin. The Freundlich isotherm model exhibits the highest level of fit as evidenced by the R^2 value of 0.99. This study offers a comparative analysis of using these natural polymers as raw materials for hydrogel synthesis and highlights their potential as efficient adsorbents for wastewater treatment applications.

Keywords: Adsorption, Hydrogels, Methylene Blue

CONTENTS

LIST OF TABLES & FIGURES

ABBREVIATIONS

XG-Xanthan Gum

LS- Lignosulfonates

KPS- Potassium persulfate

MBA- N, N′-methylene-bis-acrylamide

AA- Acrylic acid

AM- Acrylamide

MB- Methylene blue

TGA- Thermogravimetric Analysis

FTIR- Fourier Transformed Infrared spectroscopy

SEM- Scanning Electron Microscopy

XRD- X-Ray Diffraction

CHAPTER 1

INTRODUCTION

Hydrogels are three-dimensional polymeric networks that possess unique absorbent properties and retain water while maintaining their structural integrity. This water absorption capability is facilitated by the presence of hydrophilic functional groups within the polymer[1]. The cross-linking of network chains within the hydrogel structure further contributes to their stability and prevents dissolution. Due to their unique characteristics, hydrogels have found extensive applications in various fields. The ability to swell in water, biocompatibility, and hydrophilicity make them highly desirable materials. Hydrogels have been widely utilized in biological, medical, pharmacological, and environmental sciences among other disciplines[2].

Water pollution and scarcity of freshwater supplies are two of the world's most critical problems, threatening economic growth and environmental health. Industrial wastewater has received considerable attention due to its high pollution level and effective treatment challenges. Currently, dyes are used in every step of manufacturing both industrial items and consumer products. According to estimates, there are presently more than 100,000 varieties of synthetic dyes that are commercially accessible, with an estimated 700,000 tonnes of production per year. These dyes are mostly used in textiles, cosmetics, plastics, and printing industries[3]. The majority of the pollutants in textile effluent originate from the dyeing process. The textile industry produces brightly coloured, highly organic dyeing and finishing wastes. Nearly every type of dye is harmful, carcinogenic, and mutagenic, therefore it can impair human well-being[4]. Unfortunately, only a percentage of the chemicals included in dye mixtures may be used effectively in reactions. As a result, dye-containing wastewater penetrates the aquatic environment, contaminating the area's soil ecosystem and the growth of flora and fauna[3].

According to studies, the organic cationic dye methylene blue (MB) results in cyanosis, jaundice, tissue necrosis, and nerve damage, in addition to causing nausea

and vomiting. Generally, dyes have a complex structure, and their degradation in nature is usually very slow, leading to their accumulation. So, removing the dye before the effluent is discharged into natural water bodies is pivotal[1]. To minimize the detrimental effects of manufacturing and textile effluents, clean techniques with affordable prices and biodegradable adsorbents may be beneficial. Because of its inexpensiveness, efficiency, simplicity, and environmental friendliness, the adsorption technique is preferred for dye removal[5]. However, the adsorption efficiency is mainly governed by the adsorbent type. Gels can be employed as water treatment adsorbents. The term "gel" refers to a non-fluid colloidal network or polymeric network that had its entire volume enlarged by a fluid. When the fluid is water, this type of gel is known as a hydrogel[1]. Owing to their excellent water absorption, high porosity, easy handling, and facile preparation, resulting in a flexible polymeric network that helps solute diffusion through the structure, they are widely used as an adsorbent for organic dye removal from wastewater. Considering their physically distinct, 3-D structures along with their ability to expand many times their initial volume in aqueous solutions, hydrogels provide a relatively vast surface area for the adsorption of these organic dyes[3].

These hydrogels polymer backbones can be tailored to incorporate particular hydrophilic functional groups such as carboxylic acids, amines, amides, or sulphonic acids, which can act as complexing agents for dyes with opposite charges[3]. Two such natural polymers that can be used to modify the properties of hydrogels are Xanthan Gum (XG) and Lignosulphonate Sodium salt (LS)

XG is a natural polymer that has received a lot of attention in both the academic and industrial worlds. XG is an anionic polysaccharide derived from *Xanthomonas campestris*[6]. XG is considered an efficient polyelectrolyte primarily because of the presence of tuneable hydroxyl (-OH) groups in its structure. These hydroxyl groups provide XG with unique properties and functionalities. XG has been widely employed in the pharmaceutical and cosmetic industries as a suspending agent, providing stability to formulations. Additionally, it is utilized as an additive in the food industry, where it acts as a thickening agent[7]. The structural unit of XG consists of a backbone composed of β-(1→4)- linked-D-glucopyranose glycan. The alternate glucose units in the backbone possess a short branch structure, wherein a glucuronic acid molecule

is sandwiched between two mannose units. This branching structure contributes to the overall properties and functionalities of XG[8].

Lignin has gained recognition as a sustainable biomaterial owing to its polyphenolic characteristics. It possesses a complex and highly branched structure, consisting of phenolic and aliphatic hydroxyl groups. These functional groups make lignin an attractive material for various chemical modifications and reactions, enabling the development of new bio-based materials[9]. The presence of hydrophilic functional groups on the chemical structure of lignin promotes its role as a polymer for hydrogel preparation, thereby justifying its application in agriculture, water, and soil pollution treatment, and as an adsorbent product. Biocompatibility, non-toxicity, and biodegradability are inherent properties of XG and chemical modifications such as crosslinking can help us design XG and LS mixture hydrogels to be used for various applications. Due to its aromatic properties and functional groups (alcoholic and phenolic hydroxyl groups), chemical treatments such as cross-linking and graft copolymerization are needed to make LS insoluble in water and boost their adsorption properties to improve their usage for adsorbing cationic dyes[10].

The present study focuses on the synthesis of Xanthan and Lignin-based hydrogels along with their combination for a comparative MB dye adsorption study using these hydrogels.

CHAPTER-2

LITERATURE REVIEW

Hydrogels are three-dimensional networks of polymers, which can be composed of either natural or synthetic materials. One of the peculiarities of hydrogels is their high-water content, which imparts them with a significant degree of flexibility. Under physiological conditions, hydrogels can absorb and retain a substantial amount of water or biological fluids[11]. The soft and flexible nature of hydrogels makes them an ideal substance for various uses, including biomedical applications such as tissue engineering, drug delivery systems, wound dressings, and contact lenses. Additionally, hydrogels can be engineered to exhibit specific properties, such as controlled release of drugs or bioactive molecules, responsiveness to external stimuli e.g., temperature, pH, or light, and selective permeability. These characteristics further expand the range of applications for hydrogels in fields such as biosensors, actuators, and smart materials[6,7].

In recent decades, there have been significant advancements in the field of hydrogels as functional biomaterials. Initially, the biomedical application of hydrogels faced challenges such as the toxicity of crosslinking agents and difficulties in forming hydrogels under physiological conditions. However, with the progress in polymer chemistry and a better understanding of biological processes, researchers have been able to design versatile materials and develop minimally invasive therapies[12]. Fig.1 shows diverse applications of hydrogels[13].

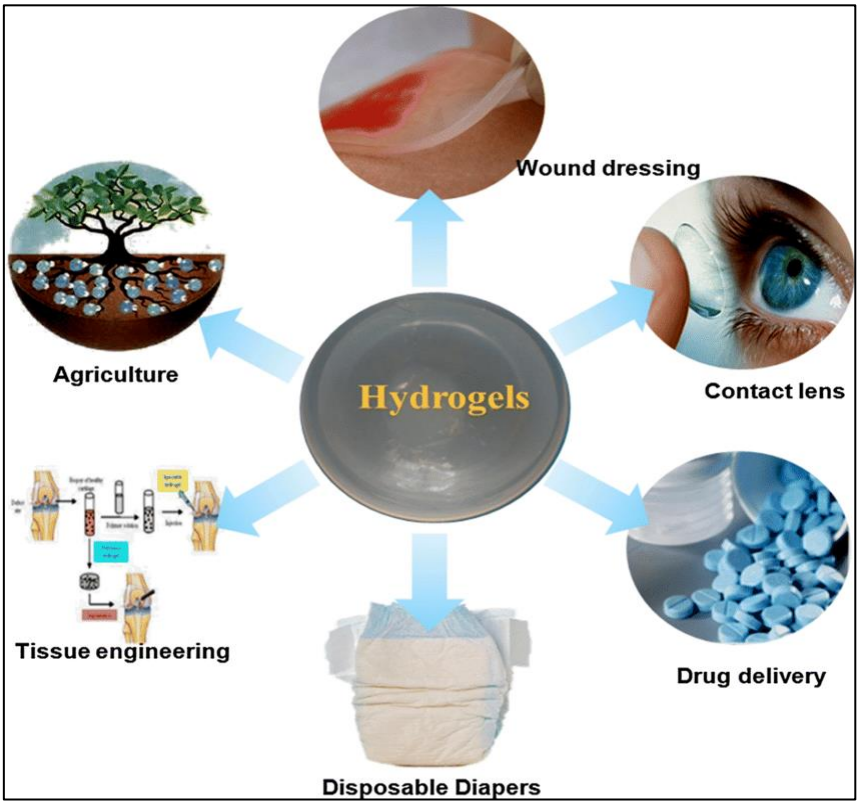

Fig.1 Applications of hydrogels

2.1 Classification of Hydrogels

Hydrogels can be classified according to their source natural or synthetic, polymer composition, cross-linking methods such as physical or chemical, ionic charge, and response to stimuli. Fig.2 shows the classification of hydrogels[14].

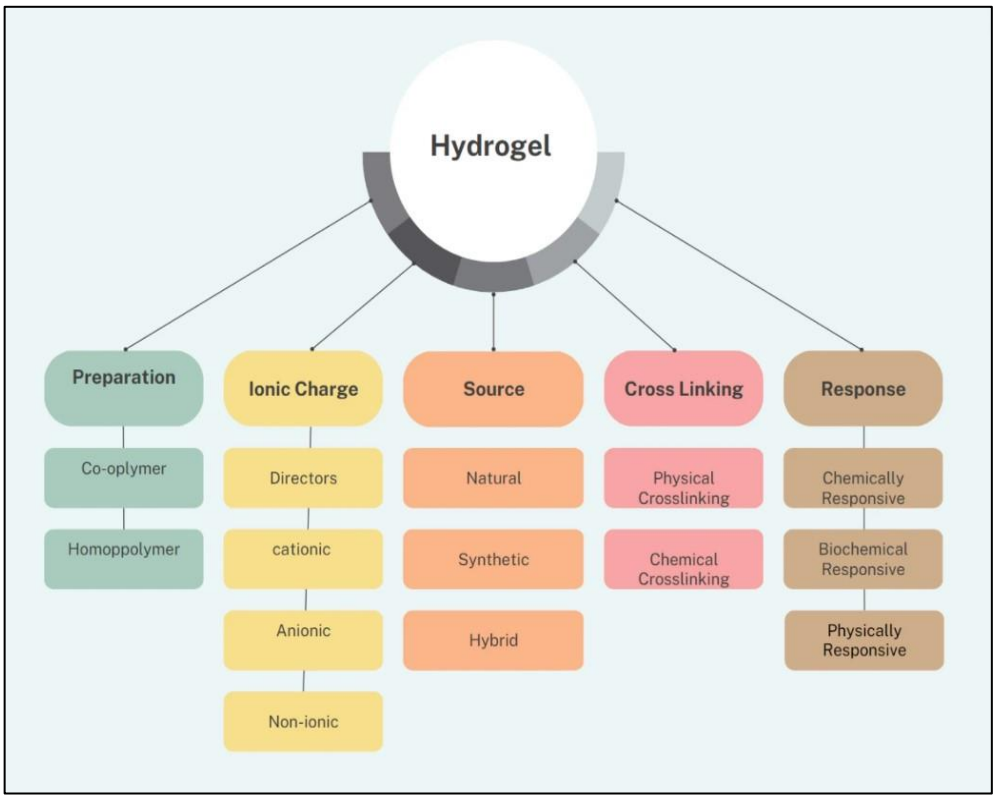

Fig.2 Classification of Hydrogels

2.2 Natural gum source

Xanthan Gum

Polysaccharides derived from renewable sources have gained significant attention due to their favorable properties such as non-toxicity, biocompatibility, biodegradability, and bio-adhesive nature. These qualities have led to their wide applications in various industries including food, pharmaceutical, biomedical, and cosmetics. Among these polysaccharides, XG has garnered particular interest over the past two decades[8]. It is a high molecular weight polymer produced through fermentation by the bacterium *Xanthomonas campestris*. The structural unit of XG consists of a backbone composed of β-(1→4)- linked-D-glucopyranose glycan, to which a trisaccharide side chain is attached. The unique chemical structure of XG contributes to its desirable properties and functionality. It imparts excellent thickening, stabilizing, and emulsifying properties. Its ability to form viscous solutions and gels in aqueous environments is particularly valuable in food formulations, where it provides texture, stability, and suspension properties[6]. Fig.3 shows the structure of XG[15].

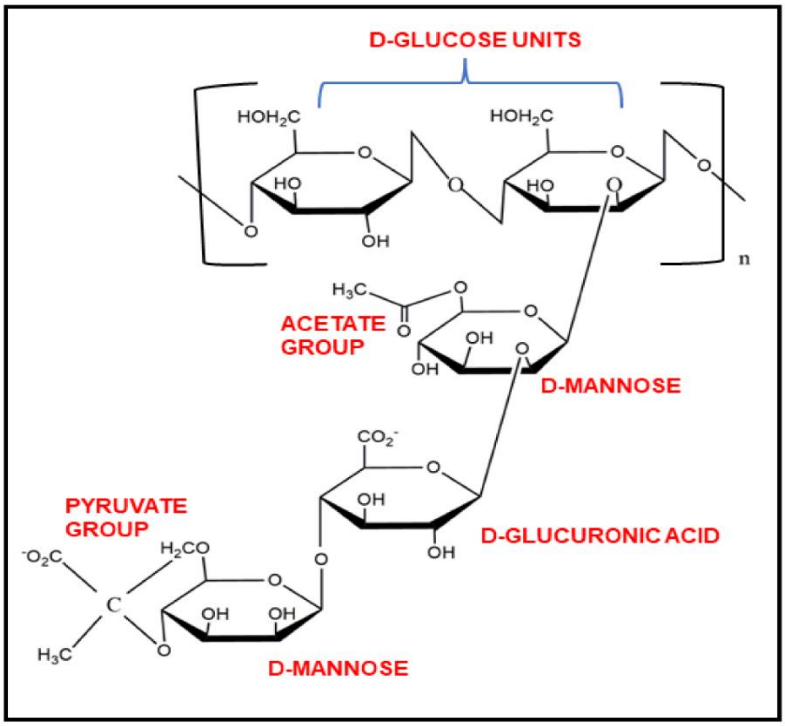

Fig.3 Chemical Structure of Xanthan Gum (XG)

2.3 Natural polymer source

Lignin

Lignin is one of the three major components that constitute the cell walls of natural lignocellulosic plants, the second most abundant and the only polyaromatic biopolymer[16]. The backbone of lignin is composed of three primary phenyl-propane monomers, which are sinapyl alcohol, coniferyl alcohol, and p-coumaryl alcohol. Fig.4 shows lignin precursors[17]. These monomers undergo enzymatic and chemical reactions, resulting in the formation of complex three-dimensional polymer networks[18].

In addition to abundance in plants, lignin is a significant by-product of the paper and pulp industry. In recent years, there has been a growing interest in utilizing lignin for the production of functional materials owing to the inherent properties of lignin such as biocompatibility, eco-friendliness, low toxicity, and sensitivity to enzymatic degradation[19]. The biocompatibility of lignin makes it suitable for use in biomedical and biomaterials. Its eco-friendliness stems from being a renewable and sustainable resource, as it is derived from plant biomass. Lignin's sensitivity to enzymatic modifications has spurred the potential use of lignin, its application, and its utilization in research and development[10].

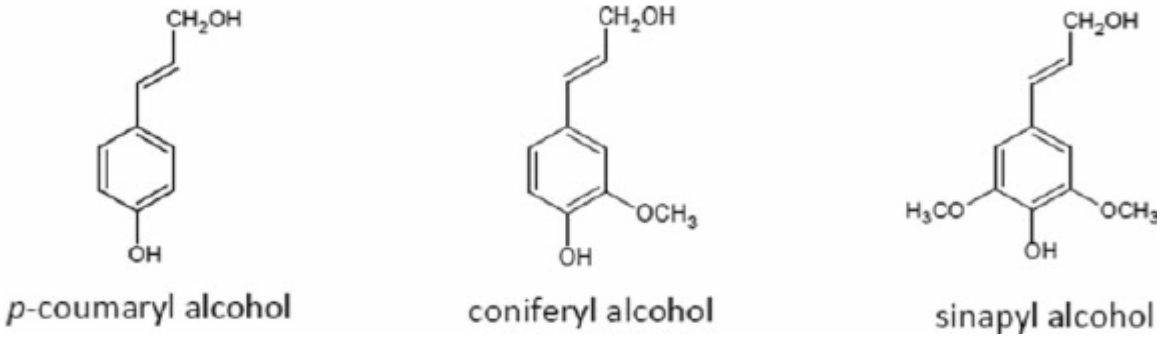

Fig.4 Lignin precursors

2.4 Xanthan gum-based hydrogel

XG is a polysaccharide that owing to its characteristic groups shows inherent behavior as a thickening agent, emulsifier, and stabilizer. Apart from this, XG also displays varied applications in drug delivery, tissue engineering scaffolds, etc. Table 1 represents already reported Xanthan gum-based materials and their applications.

Table 1 Reported Xanthan Gum based hydrogels and their applications

Source	Form	Application	References
Xanthan Gum & Starch	Hydrogel	Controlled drug delivery	[20]
Xanthan gum as a high-capacity adsorbent	Hydrogel	Dye removal	[21]
Xanthan & Sodium carboxymethyl cellulose	Interpenetrating network beads	Enhanced drug release	[22]
Xanthan Gum & soil	Matrix	Soil strengthening	[23]

2.5 Lignin-based hydrogels

The hydrogel made from natural polymers has the advantages of inherent biocompatibility and biodegradability. Bio-based hydrogels have been used in food, biomedical, cosmetics, and pharmaceutical applications. Table 2 shows lignin uses in varied fields.

Table 2 Reported Lignin-based hydrogels and their applications

Hydrogel	Application	References
Lignin	Drug-eluting antimicrobial coatings for medical materials	[24]
Lignin hydrogels and nanocomposites	Water purification and metal ion removal	[25]
Chitosan-alkali lignin	Wound healing	[26]
Lignin	Agriculture	[27]

CHAPTER 3

MATERIALS METHODOLOGY

3.1 Material

Lignosulfonic acid sodium salt (LS) was obtained from Sigma Aldrich, acrylic acid (AA) acrylamide (AM), potassium persulfate (KPS) & N, N'-methylene bisacrylamide (MBA) was obtained from Central Drug House Private Ltd., and sodium hydroxide (NaOH) was obtained from Fisher Scientific. Xanthan gum (XG) was obtained from the local market. Methylene blue dye (MB) was also obtained from Central Drug House Private Limited. All chemicals were of analytical grade and all solutions were prepared in deionized water.

3.2 Synthesis of Xanthan Gum-Based Lignin Hydrogels

In this study, XG/LS-g-PAAcoAM, XG-g-PAAcoAM, and LS-g-PAAcoAM hydrogels were synthesized through a copolymerization process using acrylic acid (AA) and acrylamide (AM) as monomers and MBA as a crosslinking agent. The synthesis process began by preparing a mixture of XG/LS (0.1 g each), AM (0.1 g), and AA, which was neutralized with an equivalent amount of NaOH. To initiate the polymerization reaction, KPS (0.1g) was added as an initiator. The reaction mixture was then stirred for 2 hours to ensure proper mixing and initiation of the polymerization process. After the initial stirring, 0.2 g MBA was added to the solution, and the reaction mixture was stirred again for 2 hours for cross-linking. The resulting solution was then transferred to a test tube and placed in a preheated water bath at 60 ℃ until the hydrogels solidified. Subsequently, hydrogels were sliced into thin pieces and immersed in distilled water to remove unreacted monomers, if any. The hydrogel was then dried in the oven at 60 ℃ and subsequently used for swelling and dye adsorption experiments. XG-g-PAAcoAM and LS-g-PAAcoAM were also prepared following the above procedure and adsorption studies were performed similarly.

3.3 Characterization

3.3.1 FTIR- Fourier transform infrared spectroscopy (FTIR) analysis was conducted using Perkin Elmer spectrum version 10.5.3 in the spectral range of 500-4000cm^{-1}.

3.3.2 SEM- The surface morphology and chemical composition of XG/LS-g-PAAcoAM, XG-g-PAAcoAM, and LS-g-PAAcoAM samples were examined using (Model: JEOL JS-6610LV). Samples were coated with gold and SEM was operated at 20 kV accelerating voltage up to 5,000x magnifications.

3.3.3 TGA- The thermo-gravimetric analysis (TGA) was performed using a PerkinElmer model TGA 4000 thermo-gravimetric analyzer under an N_2 atmosphere. The analysis involved a uniform heating rate of 10℃/min of starting from 25℃ and reaching a maximum temperature of 800℃.

3.3.4 XRD- X-ray diffraction (XRD) patterns were obtained using an Expert Pro MRD analytical X-Ray diffractometer. The diffraction angle was analyzed at 40KV in the scanning range of 5° to 80°.

UV-Visible spectrophotometer- The UV-Visible absorption spectra were recorded using a UV-1800 spectrophotometer manufactured by Shimadzu, Japan.

3.4 Swelling Index

The swelling index of the hydrogel was assessed by submerging dry hydrogel pellets of XG-g-PAAcoAM, LS-g-PAAcoAM & XG/LS-g-PAAcoAM (each weighing 0.1 g) in 200 ml of deionized water. At regular intervals, the swollen hydrogel was removed and weighed until a constant weight was attained. Excess water present on the surface of the hydrogel was gently dabbed with tissue paper. The swelling index (SI) was calculated using the formula-

$$Swelling\ index\left(\frac{g}{g}\right) = \frac{W_s - W_d}{W_s} \qquad (1)$$

where (W_s)= weight of swollen hydrogel, (W_d)= weight of dried hydrogel

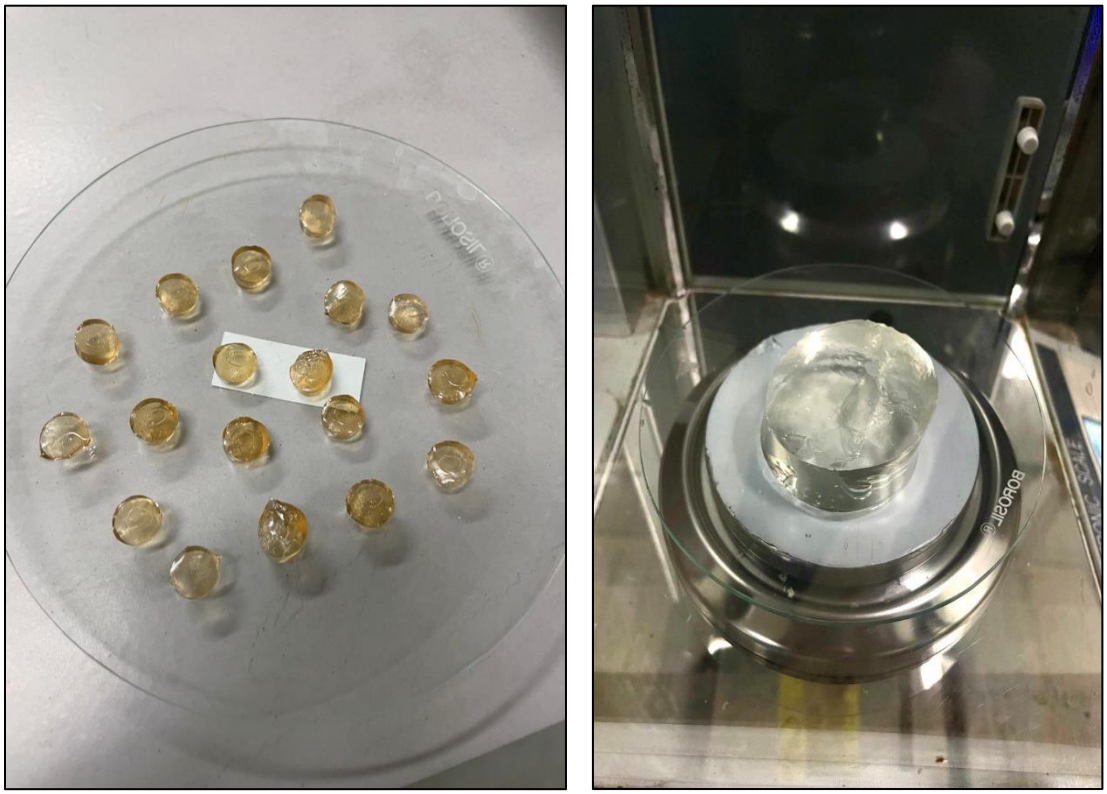

Fig.5 (a) Dried hydrogel (b) Swollen Hydrogel

3.5 Adsorption experiments

In this study, XG-g-PAAcoAM, LS-g-PAAcoAM & XG/LS-g-PAAcoAM hydrogels were employed as adsorbents to evaluate the adsorption of Methylene blue (MB) dye. The absorbance of the dye solutions was measured at Λ_{max} of 664 nm using a UV-VIS spectrophotometer. The adsorption experiments were carried out by introducing a predetermined amount of adsorbent into a 20 mL solution of MB dye, which was then stirred for 7 hours at a temperature of 25 ℃.

To estimate the percentage removal of MB dye (% R), amount of MB dye adsorbed at equilibrium (q_e), and amount of MB dye adsorbed at time t (q_t), the following equations were employed

$$\%R = C_o - C_t C_o \quad (2)$$

$$q_e = (C_o - C_e)VW \quad (3)$$

$$q_t = (C_o - C_t)VW \quad (4)$$

Where q_e and q_t stand for the amount of MB dye (mg/g) adsorbed onto adsorbents at equilibrium and at any time t, C_o (mg/L), C_t (mg/L), C_e (mg/L), W (g), and V (L) are the initial concentration, concentration at time t, equilibrium concentration, mass of adsorbent and volume of MB dye solution respectively[28].

CHAPTER 4

RESULT & DISCUSSION

4.1 Synthesis

The hydrogel used in the study was prepared by grafting acrylamide (AM) and sodium acrylate onto Xanthan Gum (XG) and lignosulfonate (LS) using potassium persulfate (KPS) as an initiator and (N, N-MBA) as a crosslinking agent. The synthesis of the hydrogels followed a free radical mechanism, where KPS, upon heating, generated free radicals that initiated the radical formation and further crosslinking of the polymeric chain was done by N, N-MBA, ultimately terminating the reaction. The interaction between the amino and carboxyl groups of AM and sodium acrylate led to the restructuring of XG molecules, resulting in the formation of hydrogels[29]. The grafting of acrylic acid and acrylamide onto LS and XG was confirmed through FT-IR studies. FT-IR analysis involves studying the infrared absorption spectra of hydrogel samples, which provides information about the chemical bond and functional groups present in the hydrogel structure. The presence of characteristic peaks in the FT-IR spectra indicates the successful grafting of AA and AM onto LS and XG, confirming the modification of the polymers and the formation of hydrogels.

Fig.6 Synthesized hydrogels

4.2 Characterisation

4.2.1 FTIR

The FT-IR spectra of XG-g-PAAcoAM, LS-g-PAAcoAM, and XG/LS-g-PAAcoAM, as shown in Fig.7, exhibit several characteristic absorption bands. These bands provide information about the functional groups and chemical bonds present in the hydrogels. One prominent absorption band observed in all three spectra is located at approximately 3307 cm^{-1}, 3305 $cm^{-1,}$ and 3308 cm^{-1}, respectively. This absorption band corresponds to the O-H stretching vibrations, indicating the presence of hydroxyl groups in the hydrogels. Additionally, there are absorption bands observed at around 2914 cm^{-1}, 2933 $cm^{-1,}$ and 2987 cm^{-1} in the spectra of XG-g-PAAcoAM, LS-g-PAAcoAM, and XG/LS-g-PAAcoAM, respectively. These bands are attributed to the C-H stretching vibrations of (-CH_2) and (-CH_3) groups, indicating the presence of alkyl chains in the hydrogels[10]. The band observed at 1028 cm^{-1} is attributed to the presence of an ether linkage in the hydrogels. The intensity of this absorption band is more pronounced in XG-g-PAAcoAM compared to LS-g-PAAcoAM and XG/LS-g-PAAcoAM. This difference in intensity can be attributed to the presence of an anomeric carbon in XG. The absorption band observed at approximately 1560 cm^{-1} can be associated with the vibrations of the aromatic skeleton. Another notable band observed in the spectra is located at around 1677 cm^{-1} in XG-g-PAAcoAM, 1670 cm^{-1} in LS-g-PAAcoAM, and 1664 cm^{-1} in XG/LS-g-PAAcoAM. This particular band corresponds to the C=O stretching vibration of the carboxylate ion, indicating the presence of carboxylate functional groups in the hydrogels[30]. These observations demonstrate that grafting occurred, resulting in the modification of the polymer structures. So, it can be concluded that XG, LS, and XG/LS are effectively grafted with AA and AM.

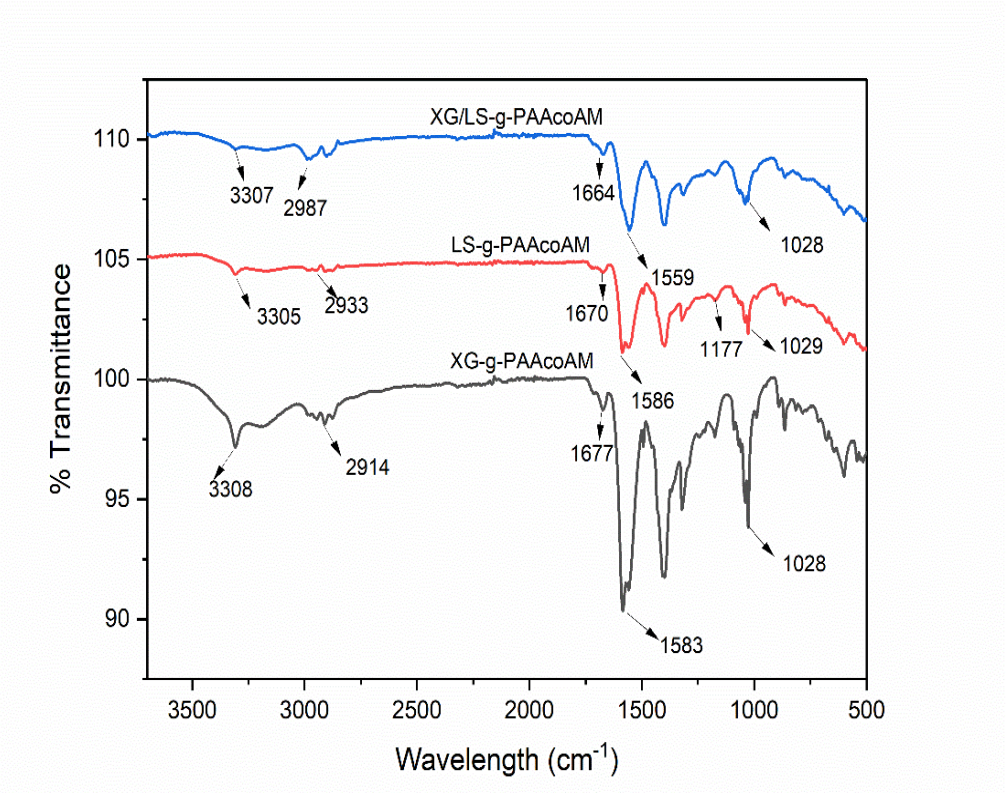

Fig.7 FTIR Analysis of XG-g-PAAcoAM, LS-g-PAAcoAM and XG/LS-g-PAAcoAM

4.2.2 SEM

The surface morphologies of XG-g-PAAcoAM, LS-g-PAAcoAM & XG/LS-g-PAAcoAM are depicted in Fig. 8 SEM micrograph of XG-g-PAAcoAM shows uneven surface morphology as shown in fig. (a) while that of LS-g-PAAcoAM shows a granular surface as shown in fig (b). In Fig (c) heterogenous, rough, granular, and porous surface is observed which further signifies that adsorption can take place easily on XG/LS-g-PAAcoAM.

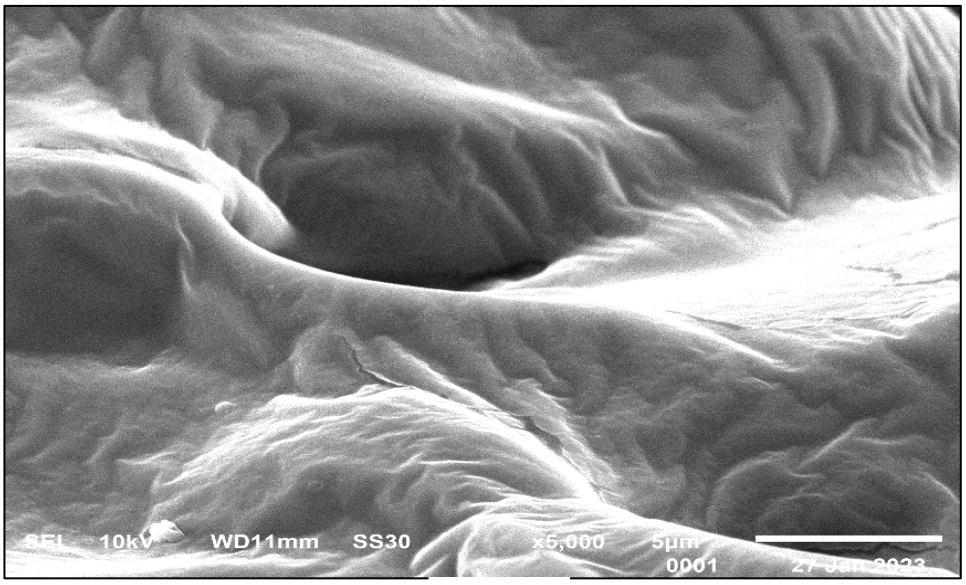

(a)

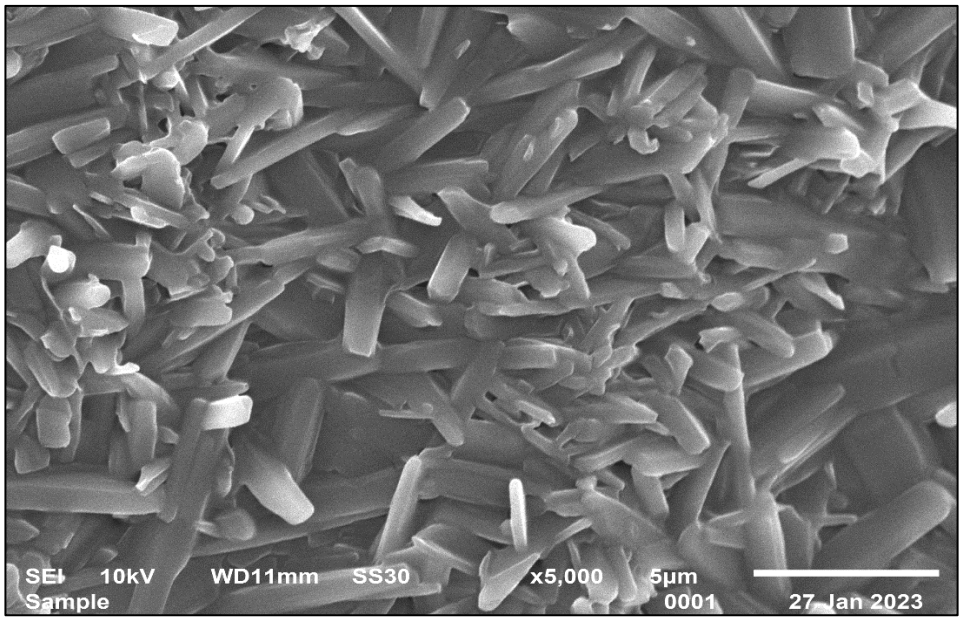

(b)

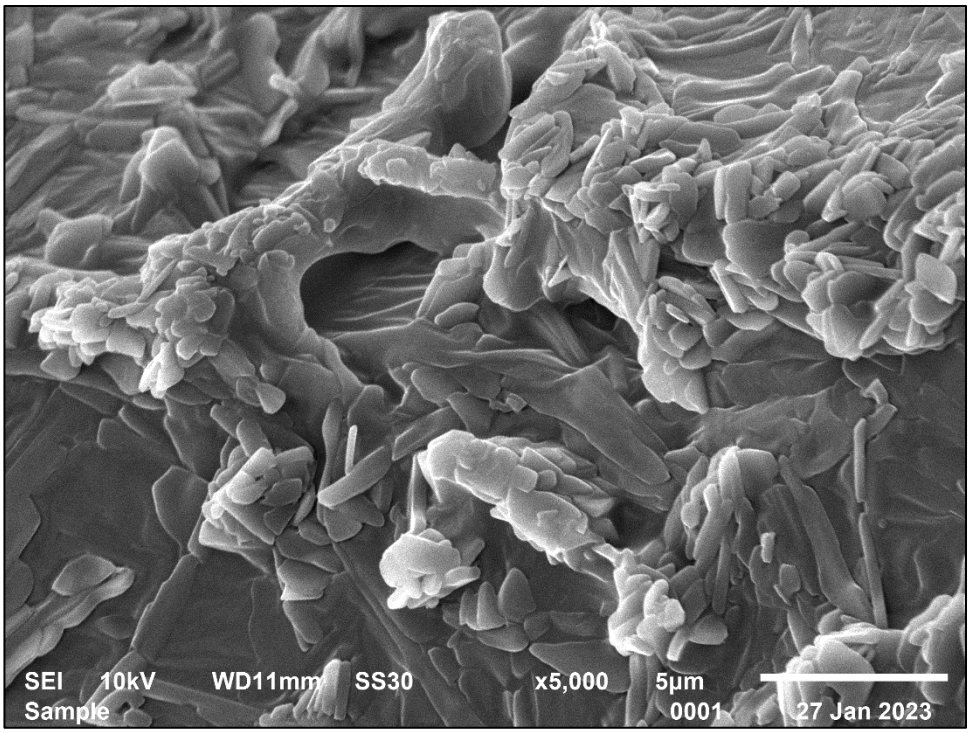

(c)

Fig.8 SEM images of (a) XG-g-PAAcoAM, (b) LS-g-PAAcoAM and (c) XG/LS-g-PAAcoAM

4.2.3 TGA

The first stage resulted in a 7% weight loss for all three hydrogels which occurred up to 250 ℃ owing to the loss of physically adsorbed water[10]. In the second stage, around 250-450 ℃, 21% weight loss occurred because of the decomposition of small molecules of LS present. The main breakdown process is shown by lignin's inclusion into xanthan forming XG/LS-g-PAAcoAM hydrogel which occurred in the temperature range of 320-450 ℃. The third mass loss step observed in the temperature range of 552 -600℃ is the range where the majority of weight loss (about 50%) occurred as shown in Fig.9. This relatively wide decomposition range indicates a slow rate of evolution of the volatile decomposition products [30]. The residual mass obtained was 53.25 %, 56.046 % & 57.829 % for XG-g-PAAcoAM, LS-g-PAAcoAM & XG/LS-g-PAAcoAM respectively. Thus, the thermally most stable hydrogel observed was XG/LS-g-PAAcoAM.

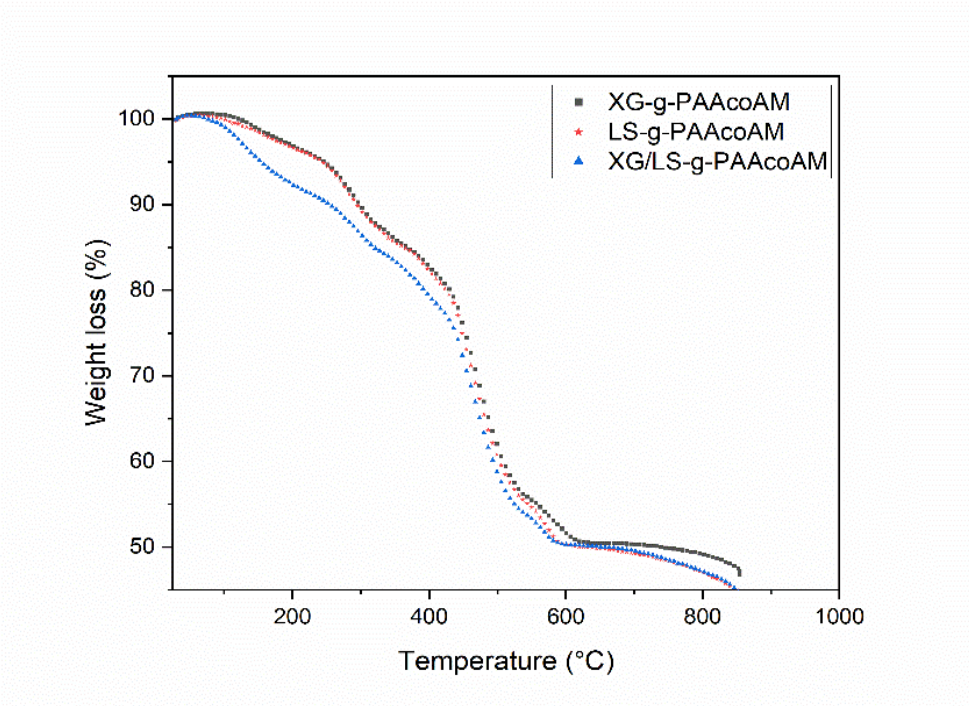

Fig.9 TGA curves of for XG-g-PAAcoAM, LS-g-PAAcoAM & XG/LS-g-PAAcoAM

4.2.4 XRD

The X-ray diffractogram analysis of the synthesized hydrogels, namely XG-g-PAAcoAM, LS-g-PAAcoAM, and XG/LS-g-PAAcoAM reveals important information about their structural characteristics as shown in Fig.10. In the X-ray diffractogram of XG-g-PAAcoAM, a broad, noisy peak is observed around 22°. This peak indicates the lack of long-range order in the hydrogel. The broadening and noise in the peak suggest the amorphous nature of XG-g-PAAcoAM hydrogel. Similarly, for XG/LS-g-PAAcoAM, a peak around 22° is also observed but with a lower intensity. In contrast, LS-g-PAAcoAM does not show any prominent peak which further confirms the amorphous nature of hydrogel. Based on the above XRD analysis, it can be concluded that none of the three synthesized hydrogels exhibit a sharp peak, indicating their amorphous nature.

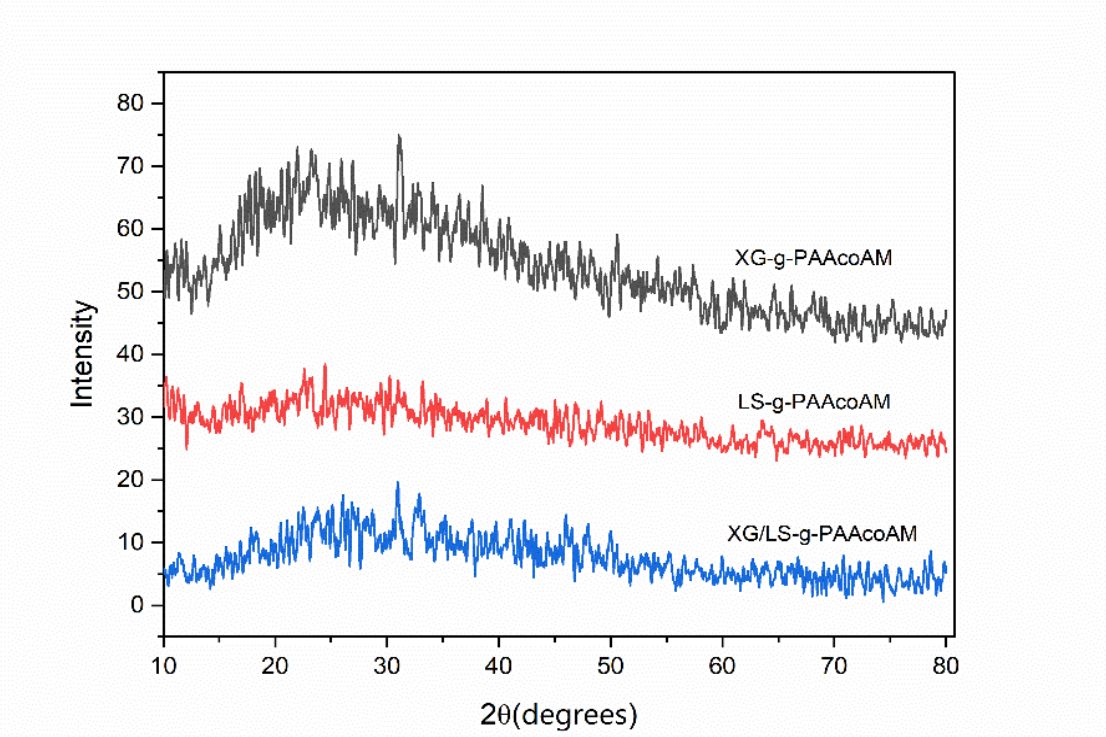

Fig.10 XRD pattern of XG-g-PAAcoAM, LS-g-PAAcoAM & XG/LS-g-PAAcoAM

4.3 Swelling Index

The swelling behavior of hydrogels was investigated in different aqueous media with pH values of 4.0, 9.0, and in deionized water (DI). The results of the swelling index (SI) are shown in Fig.11. The plot demonstrates the change in the equilibrium swelling index (SI) with varying pH levels.

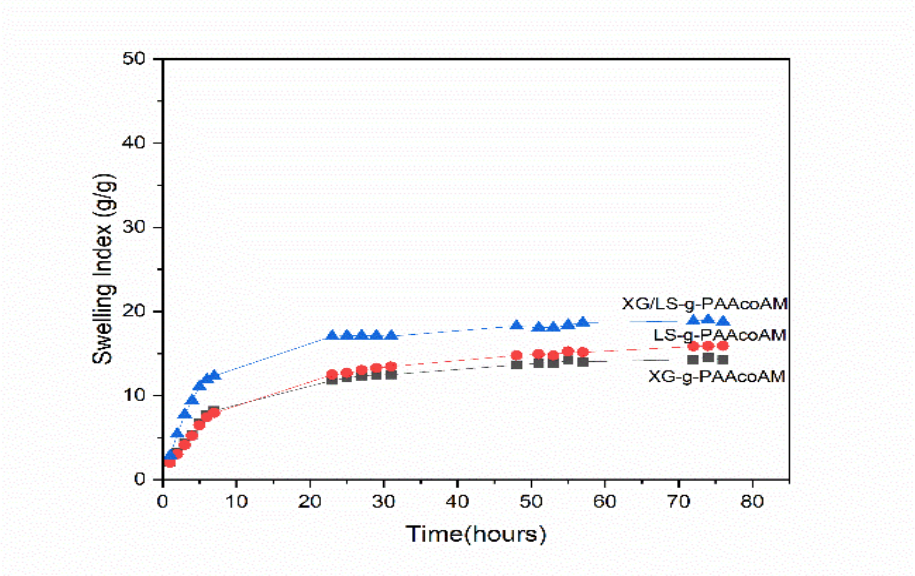

(a)

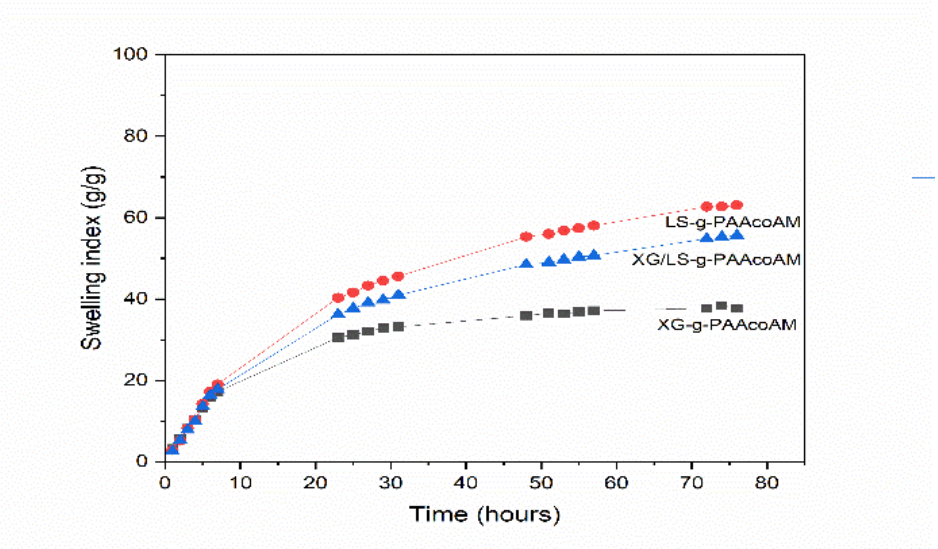

(b)

The reduced swelling of hydrogels in an acidic medium Fig. (a) may be attributed to the improper ionization of the cross-linked network. The acidic environment hinders the ionization of functional groups within the hydrogel structure, leading to reduced electrostatic repulsions and, consequently lesser swelling. Under alkaline conditions (pH 9), the presence of carboxylate ions ($-COO^-$) promotes electrostatic repulsion, creating larger gaps within the hydrogel structure. These larger interspaces allow for higher water uptake by the hydrogels, leading to increased swelling and consequently a higher SI.

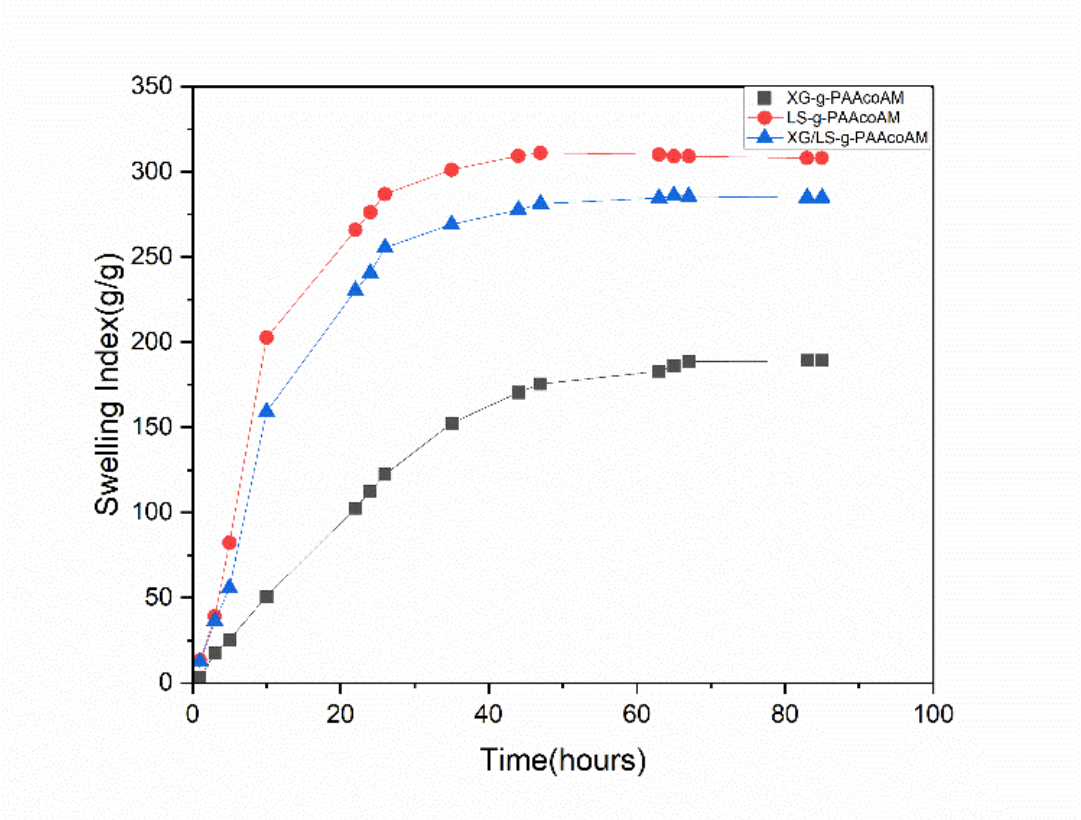

(c)

Fig.11 Swelling Index (a)At pH 4 (b) At pH 9 (c) DI

4.4 Adsorption Isotherms

Adsorption isotherms are useful in the interpretation of the distribution of adsorbate(dye) molecules between the adsorbent surface and solution phase at equilibrium. By examining the interaction between adsorbate and adsorbent, adsorption isotherms provide insights into the adsorption capacity of the adsorbent[31]. Here, Langmuir, Freundlich, and Temkin model has been deployed.

The Langmuir isotherm is a model that is suitable for describing monolayer adsorption on a homogenous site and the Langmuir isotherm's linear form is as follows-

$$\frac{1}{q_e} = \frac{1}{q_o} + \frac{1}{q_o b C_e} \qquad (5)$$

where the Langmuir constants b (L/mg) and q_o (mg/g) denote the adsorption rate and capacity, respectively. The Langmuir parameters can be determined by plotting a linear graph between $1/q_e$ and $1/C_e$ and calculating the intercept ($1/q_o$) and slope ($1/q_o b$) values. Here, C_e (mg/L) represents the equilibrium concentration, and q_e (mg/g) represents the quantity of MB dye adsorbed at equilibrium.

The dimensionless separation factor (R_L) is a parameter utilized to assess the favourability of the reaction. The interpretation of (R_L) values is given as follows-

($0<R_L,1$) indicates favourable process, ($R_L>1$) indicates unfavorable process, ($R_L=1$) indicates linear adsorption, and ($R_L=0$) indicates irreversible adsorption[32]. The equation used to calculate R_L is

$$R_L = \frac{1}{1 + bC_o} \qquad (6)$$

where C_o denotes the initial MB dye concentration.

The Freundlich isotherm model suggests that heterogeneous surfaces of adsorbents undergo multilayer adsorption. Initially, the stronger binding sites are predominantly utilized, and the strength of the binding is primarily governed by the equilibrium concentration of the adsorbates. The linear equation for Freundlich isotherm is

$$lnq_e = lnK_f + \frac{1}{n} lnC_e \qquad (7)$$

where the Freundlich constant, K_f [mg/g(L/gm)$^{1/n}$] gives an idea about bonding energy, adsorption capacity and quantity of adsorbate (MB) adsorbed at equilibrium. A value of 1/n represents adsorption intensity or surface heterogeneity and a value of n lying between 1 to 10 suggests the favourability of the adsorption process.

The Temkin isotherm describes the indirect adsorbate-adsorbate interactions and implies that, as a result of these interactions, the heat of adsorption reduces linearly with coverage. The following equation (8) represents a linear form of Temkin isotherm.

$$q = BlnA_T + BlnC_e \qquad (8)$$

$$B = \frac{RT}{b_T}$$

where equilibrium binding constant A_T represents maximum binding energy, and B is a constant that signifies adsorption heat. The linear plot of q_e against ln C_e gives slope B and intercepts $BlnA_T$ from which the value of B and A_T can be calculated[31].

Adsorption isotherm studies are significant as they offer insights into the adsorbent and adsorbate interaction. The value of the regression coefficient (R^2) of isotherm plots can be used to assess the reliability of the adsorption isotherm model by fitting experimental data to their equations. Fig.12 depicts the plots of Langmuir, Freundlich, and Temkin models and Table 3 presents the calculated parameters. From the calculated data, it may be inferred that although the experimental data for all three adsorbents fits well to Langmuir, Freundlich, and Temkin models, the best fit was observed to be with the Freundlich model, as concluded from the R^2 values found to be 0.99. The n value lying between 1 and 10 for each adsorbent hints towards the favourability of the adsorption process and it may be inferred that synthesized hydrogels can be successfully used for adsorption of MB.

Table 3: Isotherms data for (a)Langmuir (b)Freundlich (c)Temkin

(a)Langmuir isotherm data

	R^2	b	R_L
XG-g-PAAcoAM	0.9816	3.22	0.015
LS-g-PAAcoAM	0.9729	4.61	0.01
XG/LS-g-PAAcoAM	0.9811	3.08	0.015

(b) Freundlich isotherm data

	R^2	n	1/n
XG-g-PAAcoAM	0.9974	2.93	0.34
LS-g-PAAcoAM	0.9903	4.33	0.23
XG/LS-g-PAAcoAM	0.9946	2.84	0.35

(c) Temkin isotherm data

	R^2	B	A_T
XG-g-PAAcoAM	0.9873	1.64	2.71
LS-g-PAAcoAM	0.9847	2.27	2.72
XG/LS-g-PAAcoAM	0.972	2.23	2.71

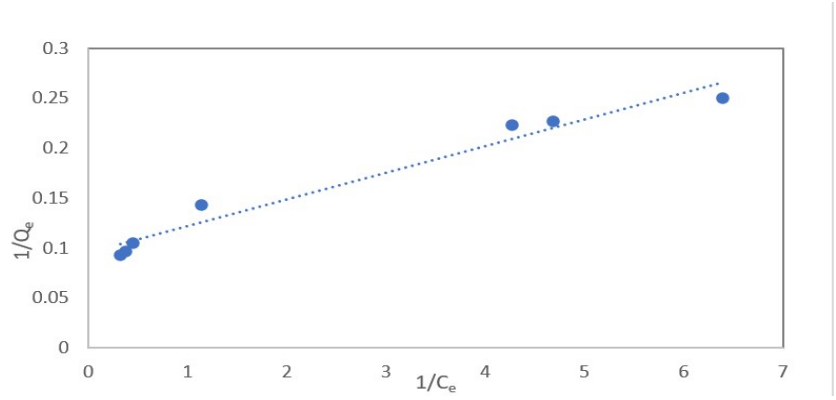

(a)

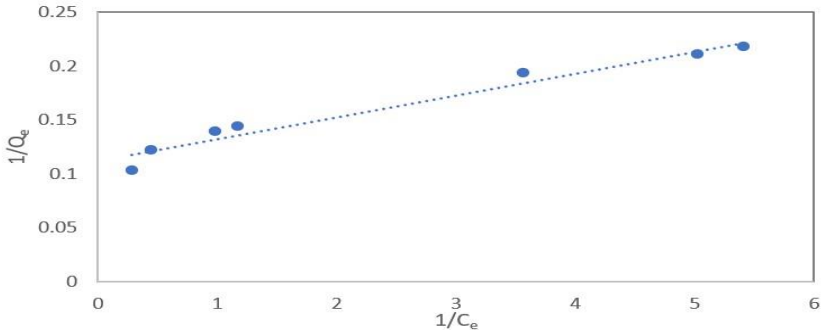

(b)

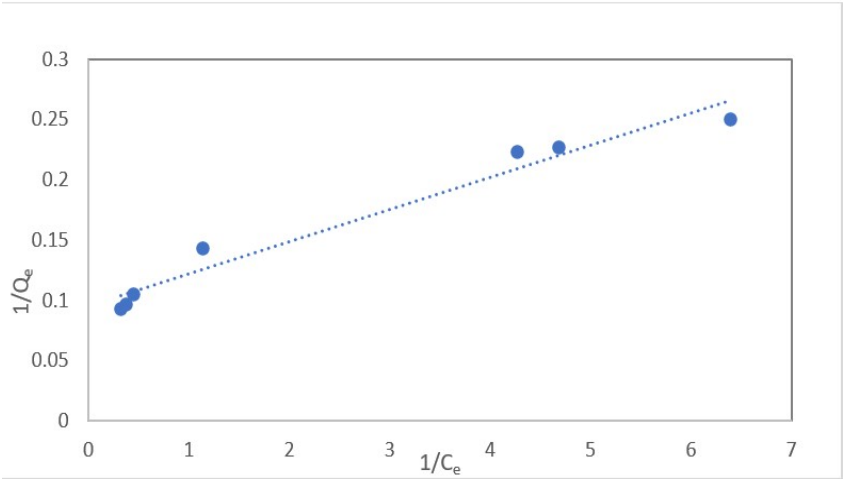

(c)

Fig. 12 (i) Langmuir isotherms graph for (a) XG-g-PAAcoAM, (b) LS-g-PAAcoAM, and (c) XG/LS-g-PAAcoAM

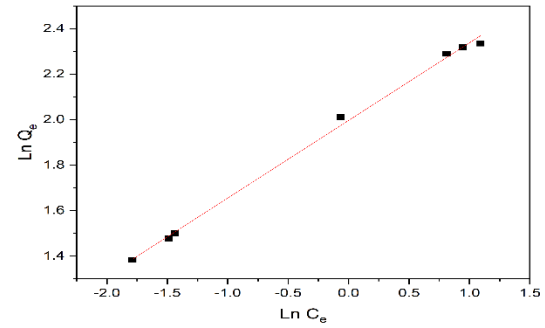

(a)

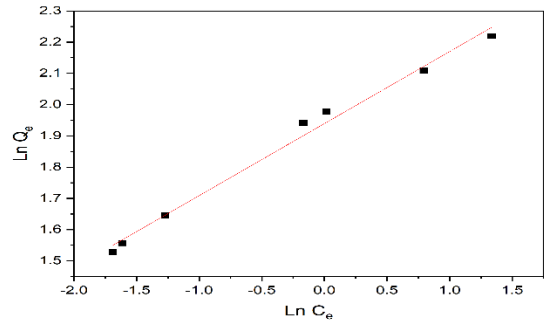

(b)

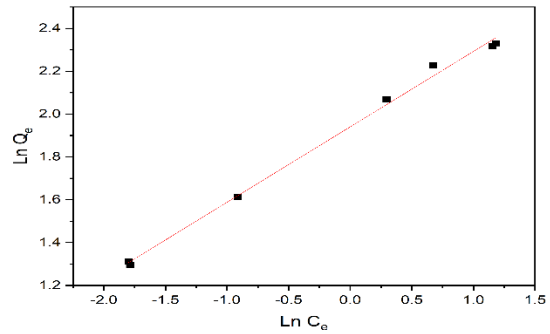

(c)

Fig.12 (ii) Freundlich isotherms graph for (a) XG-g-PAAcoAM, (b) LS-g-PAAcoAM, and (c) XG/LS-g-PAAcoAM

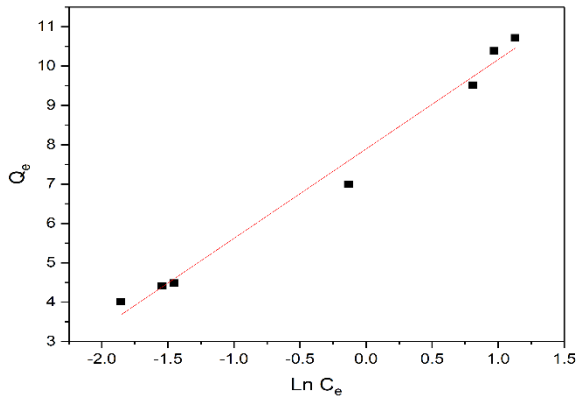

(a)

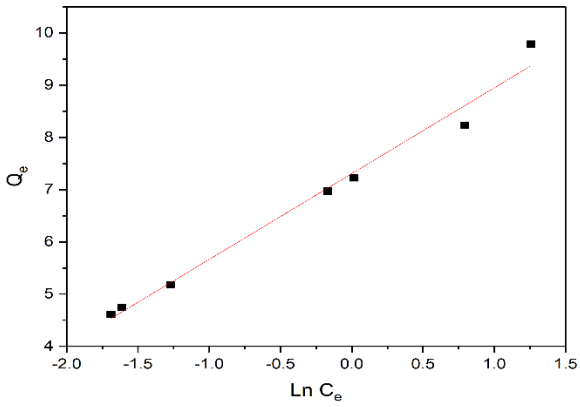

(b)

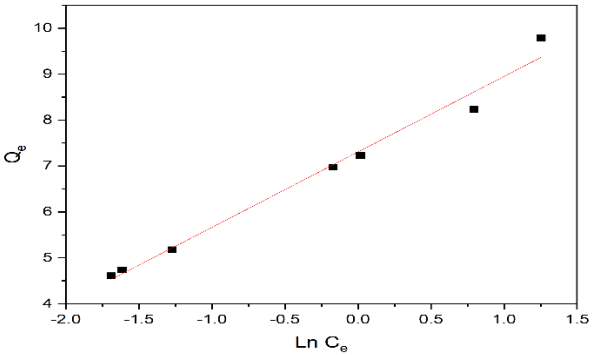

(c)

Fig.12 (iii) Temkin isotherms graph for XG-g-PAAcoAM, LS-g-PAAcoAM, and XG/LS-g-PAAcoAM

4.5 Effect of contact time on Adsorption

Contact time analysis is essential for evaluating the extent of the reaction of the adsorption process. The impact of contact duration on MB adsorption by XG/LS-g-PAAcoAM, XG-g-PAAcoAM, and LS-g-PAAcoAM hydrogel is shown in Fig.13 (a). For this study, the only variable that was changed was the contact time. All other parameters, including concentration (20 mg/L), adsorbent dose (0.20 g), temperature (30 ℃), and volume (20 mL) were held constant[31]. Fig.13 illustrates the progress of the adsorption process. It was observed that around 80% of MB was rapidly adsorbed in the first hour followed by further adsorption over the next 6 hours till adsorption reached equilibrium. At the equilibrium stage, the removal efficiency was calculated to be 91.29% for XG/LS-g-PAAcoAM, 86.5 % for XG-g-PAAcoAM, and 93.45 for LS-g-PAAcoAM. This may be explained based on competition at adsorption sites. Due to the deficiency of enough empty sites on the adsorbents, the delayed adsorption process was evident[33].

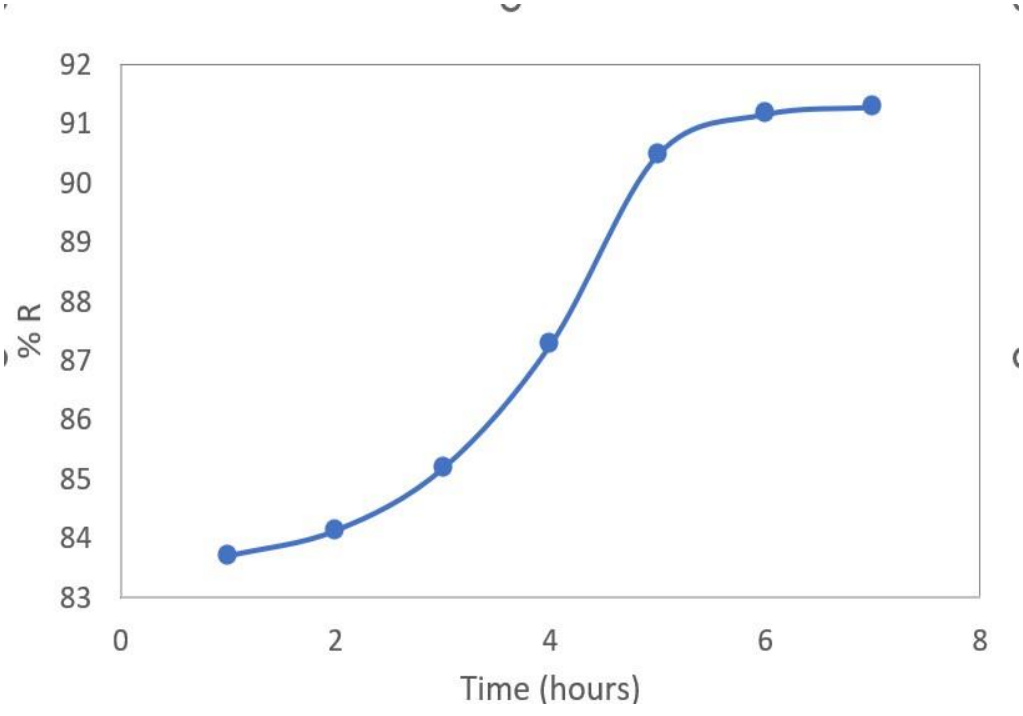

(a)

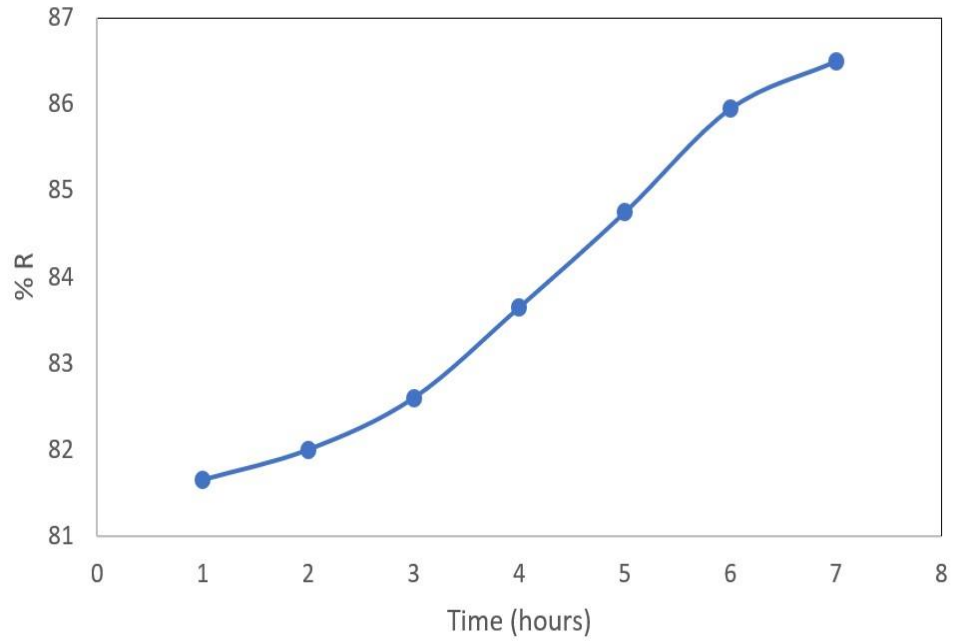

(b)

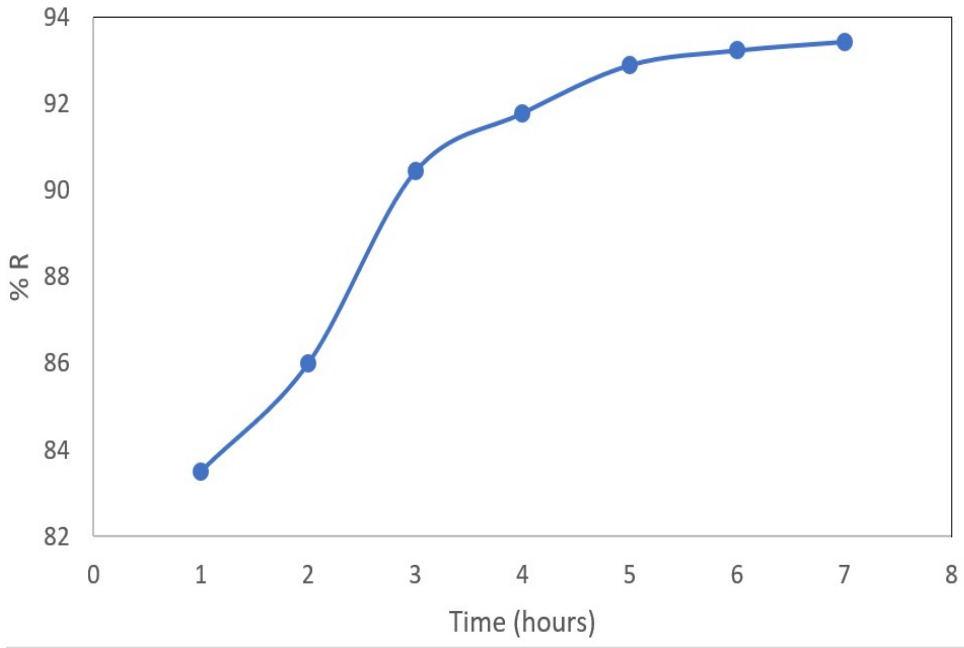

(c)

Fig.13 (a) Effect of contact time on adsorption of MB dye with a) XG/LS-g-PAAcoAM, b) XG-g-PAAcoAM, and c) LS-g-PAAcoAM hydrogel

CHAPTER 5

CONCLUSION

In the present study, we have synthesized, characterized, and performed adsorption studies through XG and LS-based hydrogels and from this study, it can be concluded that the natural polymer-based hydrogels are good sources to be used as dye adsorbent. Amongst LS-g-PAAcoAM, XG-g-PAAcoAM, and LS/XG-g-PAAcoAM hydrogels, LS-g-PAAcoAM was found to have better swelling, hence adsorption capacity and percentage dye removal. The adsorption isotherm results for synthesized hydrogels show the best fit for the Freundlich model (R^2 value = 0.99) and n was found to be well within the range 1-10 which determined adsorption to be a favorable process. The optimum parameters for maximum adsorption were found to be adsorbent dosage (0.2 g), dye concentration (20 mg/L), pH 7, temperature (300 K), and contact time (7 hours) which showed that the percentage removal efficiencies of MB were 93.45%, 86.5% and 91.29% for LS-g-PAAcoAM, XG-g-PAAcoAM, and LS/XG-g-PAAcoAM hydrogels respectively. The findings of this investigation offer compelling evidence for the potential application of LS-g-PAAcoAM as a reliable and effective adsorbent for the elimination of cationic dyes from aqueous solutions. These results highlight the promising nature of LS-g-PAAcoAM as a viable option in addressing the challenge of cationic dye removal.

REFERENCES

[1] G. Jing, L. Wang, H. Yu, W. A. Amer, and L. Zhang, "Recent progress on study of hybrid hydrogels for water treatment," *Colloids Surfaces A Physicochem. Eng. Asp.*, vol. 416, no. 1, pp. 86–94, 2013, doi: 10.1016/j.colsurfa.2012.09.043.

[2] Y. S. Jeon, J. Lei, and J. H. Kim, "Dye adsorption characteristics of alginate/polyaspartate hydrogels," *J. Ind. Eng. Chem.*, vol. 14, no. 6, pp. 726–731, 2008, doi: 10.1016/j.jiec.2008.07.007.

[3] Y. Yang *et al.*, "Hydrogels for the removal of the methylene blue dye from wastewater: a review," *Environ. Chem. Lett.*, vol. 20, no. 4, pp. 2665–2685, 2022, doi: 10.1007/s10311-022-01414-z.

[4] X. S. Hu, R. Liang, and G. Sun, "Super-adsorbent hydrogel for removal of methylene blue dye from aqueous solution," *J. Mater. Chem. A*, vol. 6, no. 36, pp. 17612–17624, 2018, doi: 10.1039/c8ta04722g.

[5] B. Salunkhe and T. P. Schuman, "Super-Adsorbent Hydrogels for Removal of Methylene Blue from Aqueous Solution: Dye Adsorption Isotherms, Kinetics, and Thermodynamic Properties," *Macromol*, vol. 1, no. 4, pp. 256–275, 2021, doi: 10.3390/macromol1040018.

[6] E. Makhado, S. Pandey, P. Nomngongo, and J. Ramontja, "Xanthan gum-cl-poly (acrylic acid) / Reduced Graphene Oxide Hydrogel Nanocomposite as Adsorbent for Dye Removal," pp. 159–164, 2017, doi: 10.17758/eares.eap1117058.

[7] F. García-Ochoa, V. E. Santos, J. A. Casas, and E. Gómez, “Xanthan gum: Production, recovery, and properties,” *Biotechnol. Adv.*, vol. 18, no. 7, pp. 549–579, 2000, doi: 10.1016/S0734-9750(00)00050-1.

[8] J. Patel, B. Maji, N. S. H. N. Moorthy, and S. Maiti, “Xanthan gum derivatives: Review of synthesis, properties and diverse applications,” *RSC Adv.*, vol. 10, no. 45, pp. 27103–27136, 2020, doi: 10.1039/d0ra04366d.

[9] Y. Meng, J. Lu, Y. Cheng, Q. Li, and H. Wang, “Lignin-based hydrogels: A review of preparation, properties, and application,” *International Journal of Biological Macromolecules*, vol. 135. Elsevier B.V., pp. 1006–1019, Aug. 15, 2019. doi: 10.1016/j.ijbiomac.2019.05.198.

[10] L. Shi, W. Liu, X. Zhang, and J. Hu, “Preparation of Lignin Sulfonate Based/Organo-Montmorillonite Composite Hydrogel for Adsorbing Methylene Blue from Aqueous Solution,” *J. Polym. Environ.*, vol. 30, no. 10, pp. 4287–4303, 2022, doi: 10.1007/s10924-022-02508-z.

[11] F. Ullah, M. B. H. Othman, F. Javed, Z. Ahmad, and H. M. Akil, “Classification, processing and application of hydrogels: A review,” *Mater. Sci. Eng. C*, vol. 57, pp. 414–433, 2015, doi: 10.1016/j.msec.2015.07.053.

[12] S. J. Buwalda, K. W. M. Boere, P. J. Dijkstra, J. Feijen, T. Vermonden, and W. E. Hennink, “Hydrogels in a historical perspective: From simple networks to smart materials,” *J. Control. Release*, vol. 190, pp. 254–273, 2014, doi: 10.1016/j.jconrel.2014.03.052.

[13] R. D. Pyarasani, T. Jayaramudu, and A. John, “Polyaniline-based conducting hydrogels,” *J. Mater. Sci.*, vol. 54, no. 2, pp. 974–996, 2019, doi:

10.1007/s10853-018-2977-x.

[14] M. M. El Sayed, “Production of Polymer Hydrogel Composites and Their Applications,” *J. Polym. Environ.*, no. 0123456789, 2023, doi: 10.1007/s10924-023-02796-z.

[15] M. Jadav, D. Pooja, D. J. Adams, and H. Kulhari, “Advances in Xanthan Gum-Based Systems for the Delivery of Therapeutic Agents,” *Pharmaceutics*, vol. 15, no. 2, pp. 1–27, 2023, doi: 10.3390/pharmaceutics15020402.

[16] Y. Meng, J. Lu, Y. Cheng, Q. Li, and H. Wang, “Lignin-based hydrogels: A review of preparation, properties, and application,” *Int. J. Biol. Macromol.*, vol. 135, pp. 1006–1019, 2019, doi: 10.1016/j.ijbiomac.2019.05.198.

[17] C. Xu, R. A. D. Arancon, J. Labidi, and R. Luque, “Lignin depolymerisation strategies: Towards valuable chemicals and fuels,” *Chem. Soc. Rev.*, vol. 43, no. 22, pp. 7485–7500, 2014, doi: 10.1039/c4cs00235k.

[18] A. Duval and M. Lawoko, “A review on lignin-based polymeric, micro- and nano-structured materials,” *React. Funct. Polym.*, vol. 85, no. September, pp. 78–96, 2014, doi: 10.1016/j.reactfunctpolym.2014.09.017.

[19] V. K. Thakur and M. K. Thakur, “Recent advances in green hydrogels from lignin: A review,” *Int. J. Biol. Macromol.*, vol. 72, pp. 834–847, 2015, doi: 10.1016/j.ijbiomac.2014.09.044.

[20] A. Shalviri, Q. Liu, M. J. Abdekhodaie, and X. Y. Wu, “Novel modified starch-xanthan gum hydrogels for controlled drug delivery: Synthesis and characterization,” *Carbohydr. Polym.*, vol. 79, no. 4, pp. 898–907, 2010, doi: 10.1016/j.carbpol.2009.10.016.

[21] D. G. Njuguna and H. Schönherr, “Xanthan Gum Hydrogels as High-Capacity Adsorbents for Dye Removal,” *ACS Appl. Polym. Mater.*, vol. 3, no. 6, pp. 3142–3152, 2021, doi: 10.1021/acsapm.1c00343.

[22] S. S. Bhattacharya, S. Shukla, S. Banerjee, P. Chowdhury, P. Chakraborty, and A. Ghosh, “Tailored IPN Hydrogel Bead of Sodium Carboxymethyl Cellulose and Sodium Carboxymethyl Xanthan Gum for Controlled Delivery of Diclofenac Sodium,” *Polym. - Plast. Technol. Eng.*, vol. 52, no. 8, pp. 795–805, 2013, doi: 10.1080/03602559.2013.763361.

[23] I. Chang, J. Im, A. K. Prasidhi, and G. C. Cho, “Effects of Xanthan gum biopolymer on soil strengthening,” *Constr. Build. Mater.*, vol. 74, no. x, pp. 65–72, 2015, doi: 10.1016/j.conbuildmat.2014.10.026.

[24] E. Larrañeta *et al.*, “Synthesis and Characterization of Lignin Hydrogels for Potential Applications as Drug Eluting Antimicrobial Coatings for Medical Materials,” *ACS Sustain. Chem. Eng.*, vol. 6, no. 7, pp. 9037–9046, 2018, doi: 10.1021/acssuschemeng.8b01371.

[25] S. Thakur, P. P. Govender, M. A. Mamo, S. Tamulevicius, Y. K. Mishra, and V. K. Thakur, “Progress in lignin hydrogels and nanocomposites for water purification: Future perspectives,” *Vacuum*, vol. 146, pp. 342–355, 2017, doi: 10.1016/j.vacuum.2017.08.011.

[26] K. Ravishankar *et al.*, “Biocompatible hydrogels of chitosan-alkali lignin for potential wound healing applications,” *Mater. Sci. Eng. C*, vol. 102, pp. 447–457, 2019, doi: 10.1016/j.msec.2019.04.038.

[27] U. M. Ahmad *et al.*, “Can lignin be transformed into agrochemicals? Recent

advances in the agricultural applications of lignin," *Ind. Crops Prod.*, vol. 170, no. April, 2021, doi: 10.1016/j.indcrop.2021.113646.

[28] Z. Yuan *et al.*, "Preparation of a poly(acrylic acid) based hydrogel with fast adsorption rate and high adsorption capacity for the removal of cationic dyes," *RSC Adv.*, vol. 9, no. 37, pp. 21075–21085, 2019, doi: 10.1039/c9ra03077h.

[29] M. Zheng *et al.*, "pH-responsive poly (xanthan gum-g-acrylamide-g-acrylic acid) hydrogel: Preparation, characterization, and application," *Carbohydr. Polym.*, vol. 210, no. January, pp. 38–46, 2019, doi: 10.1016/j.carbpol.2019.01.052.

[30] I. E. Raschip, G. E. Hitruc, C. Vasile, and M. C. Popescu, "Effect of the lignin type on the morphology and thermal properties of the xanthan/lignin hydrogels," *Int. J. Biol. Macromol.*, vol. 54, no. 1, pp. 230–237, 2013, doi: 10.1016/j.ijbiomac.2012.12.036.

[31] F. A. Khan and M. Farooqui, "Equilibrium , kinetic and thermodynamic study for the efficient removal of malachite green dye onto untreated Morus nigra L . (mulberry tree) leaves powder and its biochar," no. March, 2023, doi: 10.56042/ijct.v30i2.66355.

[32] C. E. Enyoh and B. O. Isiuku, "2,4,6-Trichlorophenol (TCP) removal from aqueous solution using Canna indica L.: kinetic, isotherm and Thermodynamic studies," *Chem. Ecol.*, vol. 37, no. 1, pp. 64–82, 2021, doi: 10.1080/02757540.2020.1821673.

[33] G. Y. Abate, D. T. A. Nguyen, A. N. Alene, D. A. Kassie, Y. A. Addiss, and S. M. Mintesinot, "Cereal based traditional beverage of tella residue (attela) as a green organic pollutant sorbent for methylene blue dye removal: Equilibrium,

kinetics and thermodynamic studies," *Indian J. Chem. Technol.*, vol. 30, no. 2, pp. 151–164, 2023, doi: 10.56042/ijct.v30i2.64532.